ORIGINAL RESEARCH

Failure Probability of Damaged RC Frame under Fire Using Markov Chain

MohammadJavad Goodarzi[1], HamidReza Tavakoli[2], Seyed Milad Hasheminejad[3], AliReza Mohseni Saravi[4], Majid Moradi*[5]

Abstract

Engineering structures are subjected to different loads during their lifetime, which may cause damage or secondary loading effects. Among loading effects on structures, explosion and earthquake may also cause fire. A damaged structure can experience a different response under fire loading in comparison to the intact structure. In addition to strength loss, damaged reinforced concrete (RC) frames may be exposed to cracking and spalling of concrete cover at various damage levels. These phenomena affect heat transfer in the structural section. In this study, Markov probability chain analysis is used to determine the probability of the occurrence of first failure in a 7-story RC frame damaged at different levels is evaluated under fire loading. The time of the first failure in structural elements is also calculated and presented for each damage level. The results show that increased damage levels in RC frame results in a greater probability of failure and reduced time of failure under fire loading scenario. The failure probability was found as zero at damage indices of 0, 0.1 and 0.2, with non-zero probabilities for greater damage indices. The framework developed in this paper outlines the performance assessment procedure for a damaged structure that is later exposed to fire loading.

Key words: Probability of Failure, Damaged RC Frame, Post-damage Fire, Markov Probability Matrix, Monte Carlo Simulation

1. Introduction

Structures are subjected to different loads during their lifetime of service. Each load creates a different response in structures. Some responses are tangible, while most responses are subtle. The daily loads applied to the structure often produce slight and intangible responses [1]. However, a few loads result in large and noticeable responses in the structure. Earthquakes, explosions, and fires are examples of loads that cause considerable responses in structures in spite of low occurrence probability [2]. Excessive loads can lead to instability, damage and collapse of structures. Each load may cause a different damage level in the structure. These damages vary from low to high [3]. In addition to direct damage, the loads can also have secondary effects.

The evaluation of the response of structures under hazard scenarios has been developed in recent years [4]. The damage to gas pipes during an earthquake and gas leak can set the structure on fire after the earthquake. The occurrence of an internal or external explosion may be accompanied by a fire [5]. What matters first of all is the safety of structure for fire prevention and, then, fire resistance of the structure [6]. The response of intact structures exposed to fire is different from the response of damaged structures.

Mousavi, Bagchi and Kodur (2008) presented a state-of-the-art review on the

*Corresponding author
Majid_Moradi68@yahoo.com

1. Department of civil engineering, Technical and vocational university (TVU), Tehran, Iran.
2. Associate Professor, faculty of Civil Engineering, University of Noshirvani, Babol, Iran.
3. Earthquake Engineering, faculty of Civil Engineering, University of Noshirvani, Babol, Iran.
4. Structure Engineering, faculty of Civil Engineering, University of Azad, Tehran, Iran.
5. PHD in Earthquake Engineering, faculty of Civil Engineering, University of Noshirvani, Babol, Iran.

Post-earthquake fire (PEF) hazard and discussed the causes, mitigation measures, and performance of building structures under this hazard [7]. Zolfaghari, Peyghaleh and Nasirzadeh (2009) tried to provide an analytical approach towards modeling sources of intra-structure ignitions and their associated uncertainties under PEF scenario[8]. Alderighi and Salvatore (2009) presented a numerical investigation for the assessment of the structural fire performance of earthquake resistant composite steel-concrete frames[9]. Keller and Pessiki (2011) described damage patterns in the sprayed fire- resistive material (SFRM) on steel moment frame beam-column assemblages owing to a strong seismic event, and the thermal consequences of this damage when exposed to post-earthquake fire[10]. Memari, Mahmoud and Ellingwood (2014) utilized finite element simulations to provide insight into the effects of earthquake initiated fires on low-, medium-, and high-rise steel moment resisting frames with reduced beam section connections which, since the Northridge earthquake of 1994, have become common in modern earthquake-resistant the design [11]. Albuquerque, Silva, Rodrigues and Silva (2018) investigated behavior of thermally restrained RC beams in case of fire[12]. Pucinotti, Bursi and Demonceau (2011) presented the performance of steel-concrete composite full strength joints endowed with concrete filled tubes, designed with a multi-objective methodology dealing with seismic actions followed by fire[13]. Moradi, Tavakoli and AbdollahZade (2019) studied sensitivity of the failure time of reinforcement concrete frame under post-earthquake fire loading[1]. Lou et a.l (2023) studied on A framework for performance-based assessment in post-earthquake fire [14]. Risco et al. (2023) hade numerical assessment of post-earthquake fire response of steel buildings [15]. Khiali et al. (2023) havd an experimental Evaluation of Post-Earthquake Fire on Reinforced Concrete Structures [16].

Despite the notable number of studies investigating post-earthquake fire scenarios, the effect of damage caused by earthquake on the structural performance of buildings under the fire loading scenario has not been sufficiently investigated. Such damage may cause notable differences in the behavior damaged reinforced concrete buildings due to the occurrence of cracking and spalling.

In this study, the failure time of RC frames in the post-damage fire scenario is investigated through a probabilistic analysis. The fundamentals of probabilistic analysis are first studied using Markov probability matrix. Then, probabilistic analysis is done for the post-damage state at each damage level. The failure probability of structural elements is evaluated under various fire loadings. Afterward, the failure time of structure is evaluated and presented for a specific damage level.

All the articles are peer-reviewed by highly acclaimed referees and this journal reserves the right to accept, reject, edit or shorten the manuscripts. In previous researches in reinforced concrete structures, most of the deterministic analysis has been done on the structural model. In this research, while using the probabilistic method and considering the uncertainties, the Monte Carlo chain has also been developed, which did not exist in the previous research. The submitted articles are not accepted if they have been formerly published or under consideration for publication anywhere else. Furthermore, the authors of the article are held responsible for the validity of the contents of the article.

2. Research methodology

2.1 Probabilistic Analysis

In this study the probability of the first failure of reinforced concrete frame elements under fire loading after the initial damage is investigated. It is assumed that the initial load is applied to the structure and then, the damaged structure is exposed to fire loading at a specific damage level, regardless of the previous loading which causes the damage.

With reasonable accuracy, it can be assumed that the response of the structure under fire loading is the same whether the fire breaks out immediately or a long time after the structure is damaged. Therefore, the response of structure depends only on the post-damage state. This condition is represented by the Markov chain. The Markov chain is a memoryless random process, in which the conditional probability distribution of next state depends only on the current state and not on previous states [17]. The memoryless feature is referred to as the Markov property.

In Figure 1, the process of creating a Markov chain or Markov matrix is shown. As shown in Figure 1, the structure reaches a certain damage level due to an initial loading and then it is exposed to fire loading. Therefore, various damage levels caused by the previous loading in the structure are considered as the current conditions of the structure.

In thermal analysis, the stability and load-carrying capacity of members under fire loading are the performance criteria [18]. If members fail under thermal loading, it means that the Markov chain leads to failure under the thermal load at the damage level i, otherwise, the chain does not form and the structure is assumed to resist the fire load.

In Figure 1, four damage states (DS) are considered, which relate to the initial state for the structure, before the fire load is applied. In this figure, DS-4 represents the ultimate damage level in structural elements (If a member failed DS-4 has been achieved.).

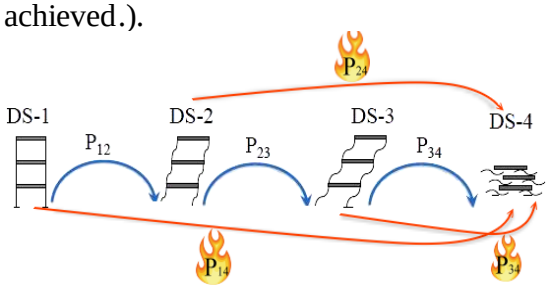

Figure 1. The process of creating a Markov chain

The structure can move from the initial damage level to a secondary damage level under different loads. For example, if a structure reaches the damage level DS-2 during the main earthquake, it can reach the damage level DS-3 due to an aftershock. Therefore, the probability of reaching the next damage level for a damaged structure by the initial earthquake can be expressed as Pij, where i is the initial damage level and j is the secondary damage level. If it is assumed that the structure is in damaged state i (DS-i), the probability of failure under fire condition is equal to Pi4. In Figure 1, a set of probabilities for moving from DS-i to DS-j in each loading can be defined according to the Markov Matrix P, which is presented in Equation (1).

$$P = \begin{bmatrix} P_{11} & P_{12} & P_{13} & P_{14} \\ 0 & P_{22} & P_{23} & P_{24} \\ 0 & 0 & P_{33} & P_{34} \\ 0 & 0 & 0 & P_{44} \end{bmatrix} \quad (1)$$

The arrays of the Markov Matrix are defined as shown in Equation (2):

$$P_{ij|A} = \int P[\,j\text{-th State}|i\text{-th State}\,]f(Z)dZ \quad (2)$$

where $P_{ij|A}$ is the probability of transferring DS-i to DS-j, provided that a specific event A occurs, $P[j-th\ state|i-th\ state]$ is the probability of at level j, provided the occurrence of damage at level i, and $f(Z)dZ$ is the occurrence rate of a specific event in a structure at damage level i.

If the fire occurs after the structural damage and it is assumed that the structure either remains intact or fails, the failure modes at different damage levels are described by matrix P_2, which is defined as follows:

$$P_2 = \begin{bmatrix} 0 & 0 & 0 & P_{14} \\ 0 & 0 & 0 & P_{24} \\ 0 & 0 & 0 & P_{34} \\ 0 & 0 & 0 & P_{44} \end{bmatrix} \quad (3)$$

Where the arrays in the fourth column represent the probability of failure under fire loading if the structure is at a specific damage level. In other words, the arrays of each column indicate the probability of failure under fire load, provided there is certain damage in the structure. In the Markov matrix, each array indicates a

conditional probability. The conditional failure probability under fire is defined by Equation 4, provided the initial damage exists at DS-i:

$$P_{i\_failure} = \int P[\,failure\ State \mid i\text{–}th\ State\,]\, f(Z)\, dZ \quad (4)$$

Where $P_{i-failure}$ is the failure probability in a structure at DS-i under fire, $P[failure\ state|i-th\ state]$ is the failure probability due to fire in a structure at DS-i and $f(Z)\,dZ$ represents the occurrence rate of fire in a structure at DS-i, which is a statistical phrase. In the equation (4), $P[failure\ state|i-th\ state]$ is an engineering term that describes the fragility of a structure under fire load conditions. In this case, each damage level can be considered as an intensity measure. If the fire load is applied for the time T and the structural failure of elements occurs at the time t, the failure probability due to fire in the DS-i is given by Equation 5:

$$P[\,failure\ State \mid i\text{–}th\ State\,] = P[t < T \mid i\text{–}th\ State\,] \quad (5)$$

Equation 5 presents the fragility of elements under the fire load if the damage level is considered as an intensity measure. Moreover, the failure probability at a specific time, e.g. t_0, is defined using Equation 6:

$$P_{failure-time} = P[t = t_0 \mid i = I] \quad (6)$$

If the damage is assumed constant, another perspective to the fragility of the structure can be obtained by taking the time under fire loading as the intensity measure. In this case, the fragility curve is found by determining the failure probability when assuming different times of exposure to fire loading.

The research process used in this study is illustrated in Figure 2. As shown in the figure, for the 7-story RC frame considered as the case study, the fragility curve based on failure time was obtained initially for a case of natural fire load [19] and the standard fire load according to ISO 834. Next, the failure probability of the building at each damage level for a specific range of damage index under fire loads is determined.

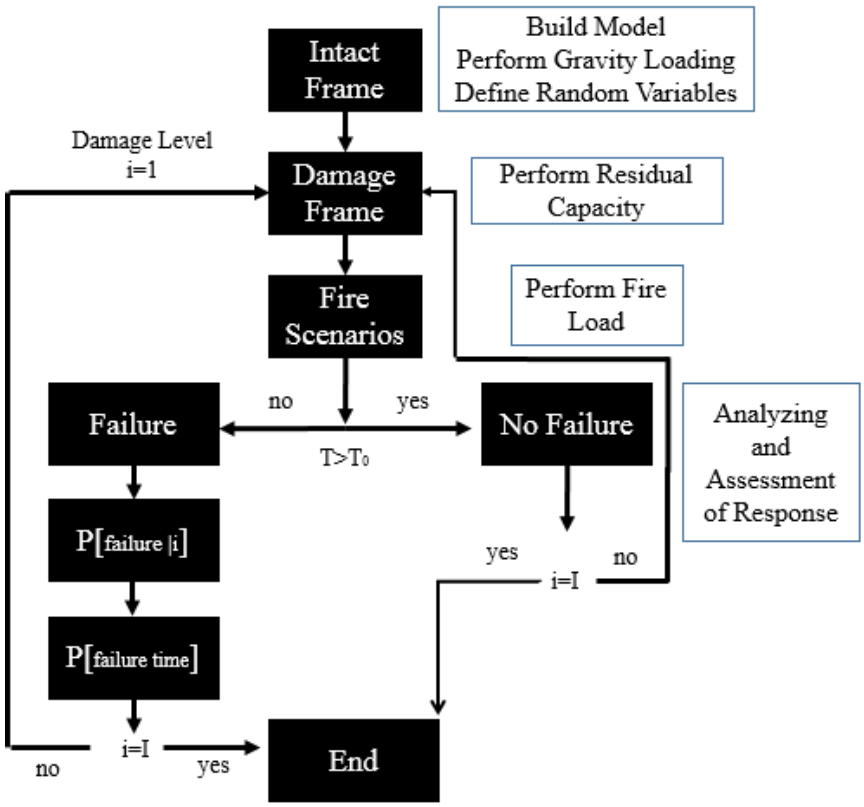

Figure 2. Steps of probabilistic analysis

2.2 Damage Index and Damage level

Damage to the structure caused by lateral loads, particularly seismic loads, is represented both quantitatively and qualitatively. Qualitative presentation of structural damage is usually done by damage level, while they are quantitatively presented by damage index [20]. The structural damages is classified in 6 damage levels, as listed in Table 1. A variety of methods are proposed for quantitative presentation and calculation of structural damage, among which modal strain energy (MSE) method and Park-Ang damage index can be mentioned [21].

Table 1. Different damage levels

Damage level	Description of damage	Damaged Index
0	No damage	0
I	Visible narrow cracks on the concrete surface (crack width is less than 0.2 mm)	0.1
II	Visible clear cracks on the concrete surface (crack width is 0.2–1.0 mm)	0.2-0.3
III	Local crushing of cover concrete Significant wide cracks (crack width is 1.0–2.0 mm)	0.4-0.5
IV	Significant crushing of concrete with reinforcing bar exposure Spalling of concrete cover (crack width exceeds 2.0 mm)	0.6-0.7
V	Buckling of the reinforcing bars Significant damage to the core concrete Visible vertical and/or lateral deformation of the column Visible settlement and/or leaning of the building	>0.8

In RC structures, the reduction of load-carrying capacity of RC elements results in cracking in concrete and yielding and possibly buckling of reinforcement (in high damage index). In this study, the concrete cracking and reduction of load-carrying capacity of RC elements are considered as two parameters influenced by damage at different levels. The effect of cracking is considered only on the heat transfer analysis in RC sections and the impact of reduction of strength is considered in mechanical-thermal analyses. Also, the damage index is considered as an intensity measure in this study.

3. Modeling

3.1 Reinforced Concrete (RC) Frame

A 7-story two-dimensional RC moment frame is used for mechanical-thermal analysis in this study. At first, a three-dimensional structure with a square plan and four, 4-m spans was considered and designed (Fig. 3). The story height was taken as 3 meters. The dead load of 600 Kg/m^2, live load of 200 Kg/m^2 and snow load of 150 kg/m^2 were assumed for the structural design. For lateral loading, according to the Iranian Seismic Code (Standard No.2800), it is assumed that structure is located in a zone of very high seismic risk. Design peak ground acceleration (PGA) was taken as considered 0.35g. The Iranian Instructions for Design of RC Structures is used for the design of the structure.

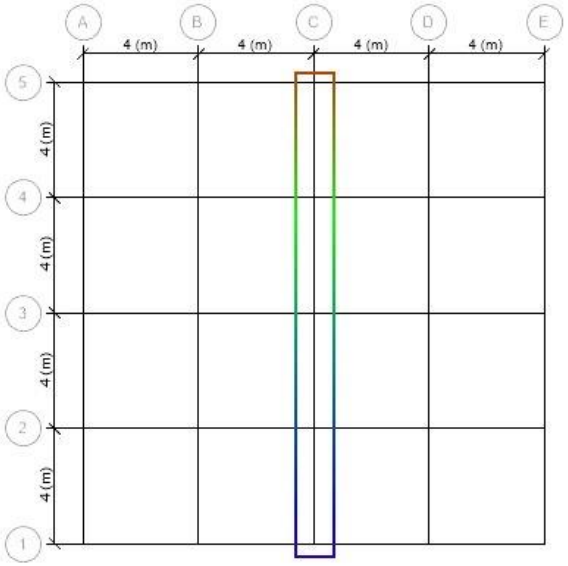

Figure 3. Plan of the structure

The concrete ultimate strength (f_c) and ultimate strength of reinforcement (f_{us}) were taken as 21 MPa and 338 MPa, respectively. The results of design are shown in Table 2. After the design, the middle frame (frame C in Figure 3) was selected from the structures for mechanical and thermal analyses.

Table 2. Structural steel sections

	Beam	Column

Story	b (m)	Bottom Rebar	Top Rebar	b (m)	**Rebar**
1	45	8 d20	7 d20	70	20 d22
2	45	8 d20	7 d20	70	20 d22
3	45	8 d16	6 d16	60	18 d20
4	40	7 d 16	6 d16	50	20 d18
5	35	7 d 12	6 d 12	50	20 d18
6	35	7 d 12	5 d 12	35	18 d16
7	35	5 d 12	4 d 12	35	18 d16

3-2- Heat Transfer

Heat transfer analysis of sections depends on a variety of factors. Density, heat transfer coefficient and specific heat capacity are the most important parameters of heat transfer in various materials. In this study, the parameters of thermal conductivity and specific heat capacity are considered as a function of temperature. In Figure 4, the values of thermal conductivity and specific heat capacity of concrete materials are shown. The density of concrete materials is taken as 2.4 g/cm3.

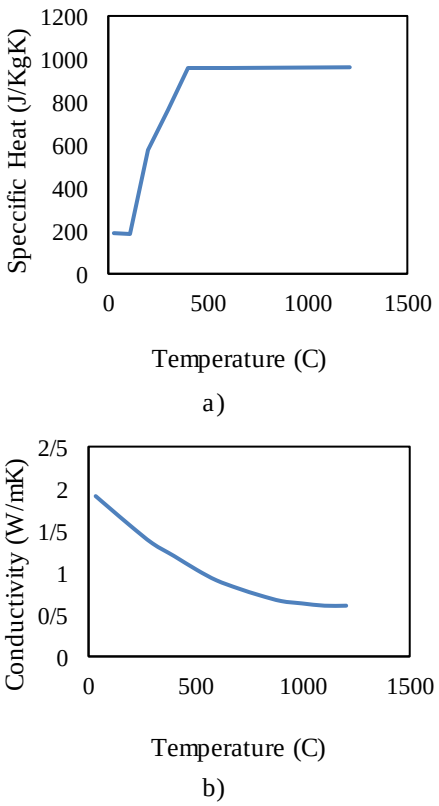

Figure 4. Changes in the thermal properties of concrete materials as a function of temperature: a) specific heat capacity; b) thermal conductivity coefficient

In order to perform the heat transfer analysis of structural sections, all structural sections presented in Table 2 were modeled using Abaqus; then, the parameters of thermal conductivity, density, and specific heat capacity are modeled within the software and the heat transfer is investigated in the sections after determining the fire load. RC section was analysis by film coefficient 25 W/m2C and emissivity 0.7 according to [22]. The beam and column sections (Table 2) were modeled and analyzed under heat transfer using Abaqus for intact and damaged models, taking into account different values of cracking at each damage level (Table 1).

The temperature-time curves are extracted for different fire loads at various heights (Section 3-4). Figure 5 shows an example of heat transfer in RC sections with small cracks and numerous cracks for the fire load presented by the standard fire load (for 5 hours). At level II, small cracks are placed in the area of the cover. At level III, deep cracks are placed in the cover area. At level IV, assuming that the cover is lost (spalling), the boundary of thermal load is transferred to the reinforcement.

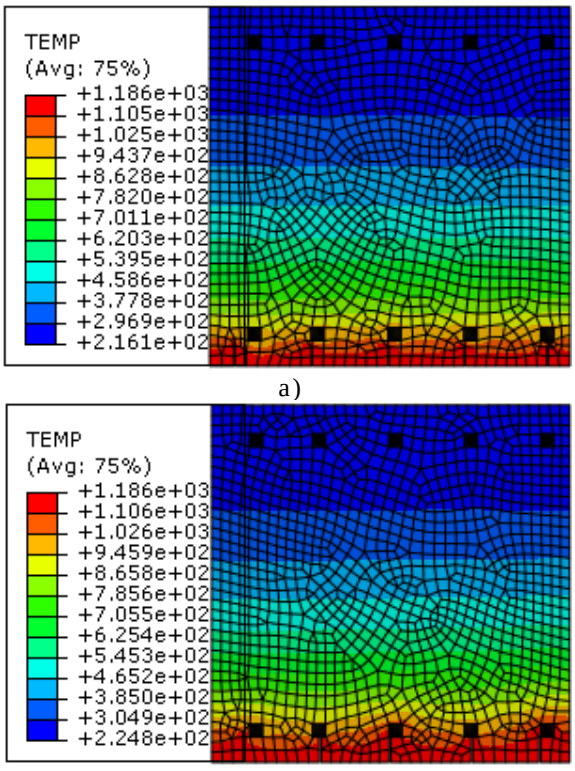

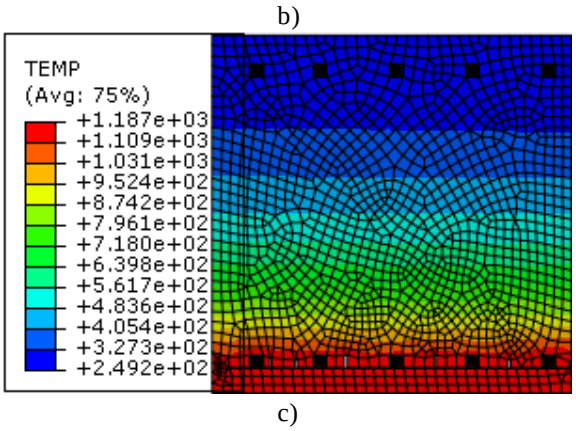

Figure 5. Heat Transfer in the concrete section under standard ISO 834 fire load: a) II b) III c) IV damage level

In this study, the effect of cracking and spalling caused by a seismic load on heat transfer analysis in reinforced concrete sections is considered [23, 24]. Table 1 is used to determine the dimensions of the crack and the presence of spalling. The effect of the cracks in the heat transfer analysis has been applied in the areas of the plastic hinges. These cracks have been created due to the initial load and its effect has only been observed in the boundary conditions of the heat transfer analysis. Spalling location is considered based on Wen et al. (2015). In this research, based on Wen et al. and behnam et al. studies, the Spalling effect (caused by the seismic load) is only intended to accelerate heat transfer. In fact, the effect of spalling is considered via transferring the boundary from the cover to the reinforcement. Therefore, the effect of spalling due to fire has not been considered in this study.

When the heat transfer analysis is conducted for different RC sections, the temperature-time curves are extracted and used for the analysis by OpenSees. In Fig. 6, the temperature-time curve extracted for the upper and lower reinforcement of the beam cross section is shown.

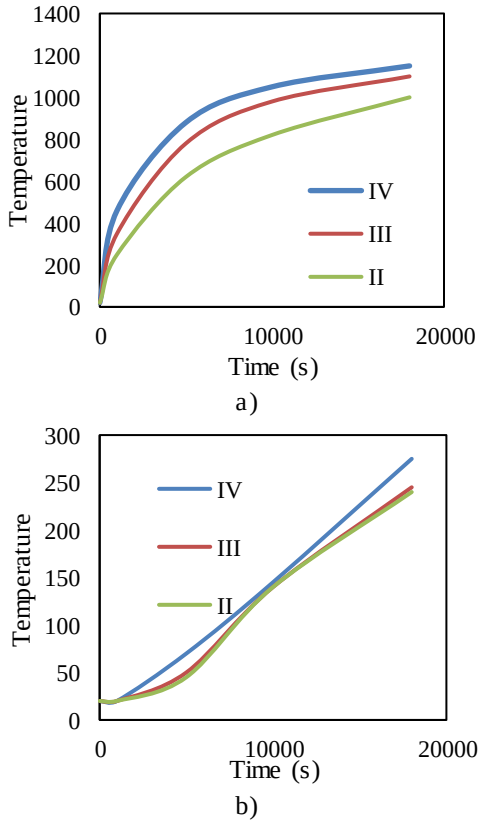

Figure 6. Temperature-time curves for different damage level, a) lower b) upper reinforcement under standard fire time-temperature curve

3.3 Mechanical-Thermal modeling and Verification

In this study, OpenSees is employed to perform the mechanical-thermal analysis in intact and damaged structures. The thermal module in OpenSees was developed by [25] for thermal analyses and fire loading. In fact, this additional feature enables the software to perform thermal and mechanical-thermal analyses. In this study, thermal and mechanical-thermal models are developed using the framework suggested by the [26]. In this software, steel thermal materials are presented as Steel01thermal and Steel02thermal, while concrete thermal materials are represented as Concrete02thermal. In accordance with EN 1992-1-2, the strength of reinforced concrete and steel is reduced as the temperature rises. The strength of concrete at elevated temperatures can be calculated using Equation 7 [27].

$$\sigma=\frac{3\varepsilon f_{c,\theta}}{\varepsilon_{c1,\theta}(2+[\frac{\varepsilon}{\varepsilon_{c1,\theta}}]^3)} \quad (7)$$

Where

σ: stress

$\varepsilon_{c1,\theta}$: $\varepsilon_{c1,\theta}$ concrete strain corresponding to $f_{c,\theta}$

$f_{c,\theta}$: the characteristic value of the compressive strength of concrete at temperature θ

ε: strain

It is observed that the strength of concrete at various temperatures is a function of the concrete ultimate strength, strain and ultimate strain at different temperatures. But in damaged concrete, the strength of concrete is different from the equation (7). In thermal loading, the initial strength of damaged RC element is replaced with the residual strength. According to the [28], the residual strength of damaged elements can be considered as a function of the damage index. Consequently, the residual strength and elastic modulus of concrete are expressed as Equation 8:

$$E_d = (1-D)E_0 \quad (8)$$

$$\sigma_d = (1-D)\sigma_0$$

Where E_d is the residual elastic modulus, E_0 is the initial elastic modulus, σ_d is the residual stress, σ_0 is the initial stress and D is the damage index. Therefore, the stress-strain relationship for a damaged element under thermal loading ($\sigma_{d,\theta}$) can be expressed as follows:

$$\sigma_{d,\theta} = \frac{3\varepsilon f_{c,\theta}}{\varepsilon_{c1,\theta}(2+[\frac{\varepsilon}{\varepsilon_{c1,\theta}}]^3)}(1-D) \quad (9)$$

The parameters of elastic modulus and ultimate stress are modified for RC materials at each damage level and the elements are then exposed to thermal loading.

The Kamath et al. (2015) [29] experimental model was used to validate the heat transfer analysis and the response of the damaged structure under fire condition. Kamath et al. subjected a three-dimensional reinforced concrete model under cyclic loading and then applied a fire load. The hysteresis curve of the numerical model (in present study) and the Kamath experimentally model are shown in Fig. 7. The moment-rotation (Fig. 8) curve of one of the columns is extracted from the numerical model and its damage index is calculated based on the Park-Ang method.

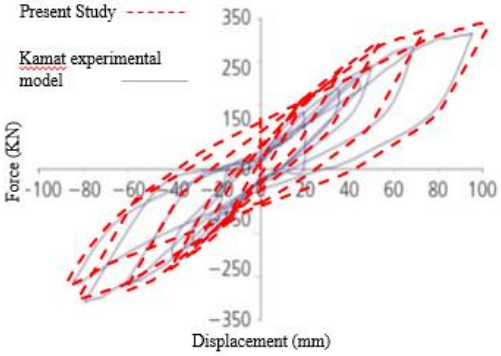

Figure 7. Comparison of hysteresis curve in Kamat model [29] and present study

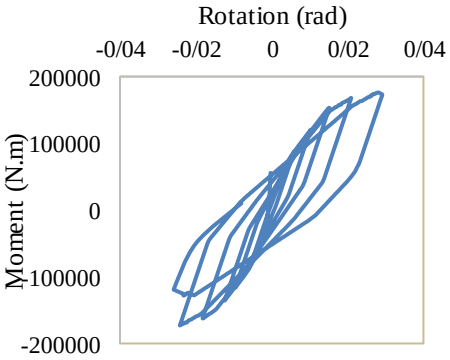

Figure 8. Column hysteresis curve

The damage index is calculated as 0.55 (damaged state III). The cracks in reinforced concrete section are applied according to Table 1 and then the RC section is subjected to heat transfer analysis. The temperature – time curves in this section were extracted and compared with the Kamath experimental model (Fig. 9). The results of the heat transfer analysis show that there is good agreement between the results of the present study and Kamath's research.

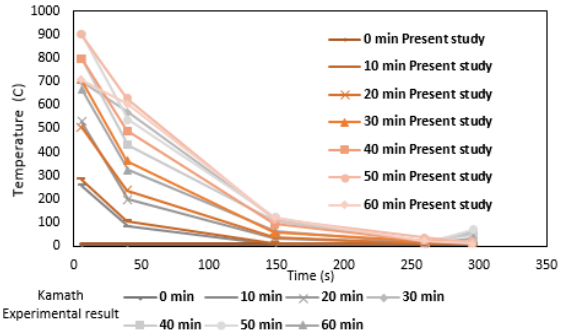

Figure 9. Comparison of heat transfer analysis results in the present study with a Kamath experimental model

The Sharma model was used to evaluate the response of damaged structures exposed to fire. Sharma has presented a numerical model from the Kamath experimental model and examined the response of RC frame in post-cyclic fire load. After finite element modeling, the structure was subjected to cyclic loading. Damage indices were calculated and applied to the structural element. Finally, fire load was applied to the structure and the vertical displacement of the middle span (Figure 10) was extracted and compared with the Sharma numerical model. The results show that there is a good agreement between the numerical model of the present study and the Sharma model.

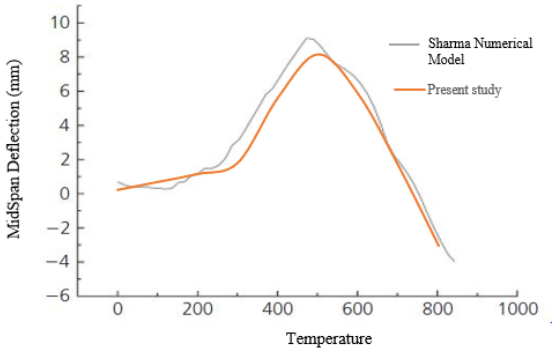

Figure 10. Comparison of Structural Response in Numerical Model of the Present Study and Sharma Numerical Model

In order to verify the failure time in post-damage fire scenario, an experimental model is numerically modeled and analyzed in accordance with the Imani et al. (2014) experimental model [30]. In this study, the experimental model proposed by Imani is used for the validation. They exposed a ductile concrete-filled double-skin tube column to cyclic loads as load control and then applied the fire loads. Afterward, they assessed vertical displacements and durability during the thermal loading. Figure 11 graphically illustrates Imani's experimental model:

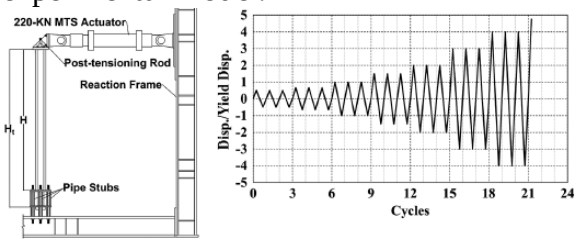

Figure 11. Imani's experimental model

The mechanical-thermal materials of Concrete02Thermal and Steel02Thermal are employed as concrete and steel materials for the modeling of this composite column. The dispBeamColumnThermal is used for the elements with mechanical-thermal properties. The column is modeled and loaded in accordance with the Imani (2014) experimental model. The results of cyclic analysis of this column under lateral loading are shown in Figure 12. In this study, the results of nonlinear mechanical analysis demonstrate that the base shear-drift curves have good agreement for both Imani's experimental models and the numerical model in this study.

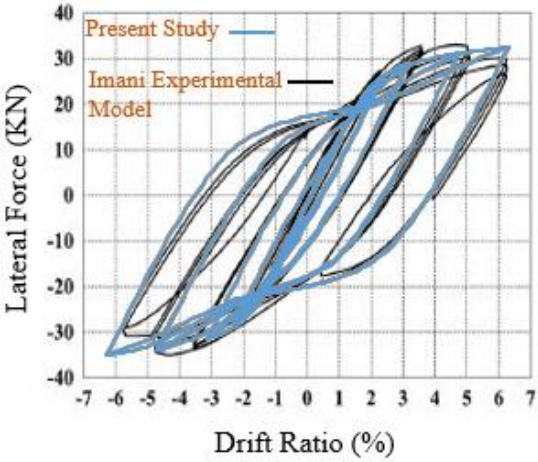

Figure 12. Hysteresis curve in Imani's experimental model and the numerical model in this study

Then, damage index has been calculated and strength has been reduced for base of column. The numerical model is exposed to thermal loading without cyclic analysis (with ultimate stress and elastic modulus modified). Figure 13 shows the vertical

displacement-time curves for the experimental model and the numerical model in this study. The results of numerical modeling in this study show that the vertical displacement of column within the range of vertical displacements in various gauges for the top of the column in an experimental model and the failure time in the numerical model of this study is accurate enough compared to Imani's experimental model. The vertical displacement in the numerical model is close to the mean value of gauges 1 and 2 in the Imani experimental model (Fig. 13), which indicates the accuracy of numerical results in this study.

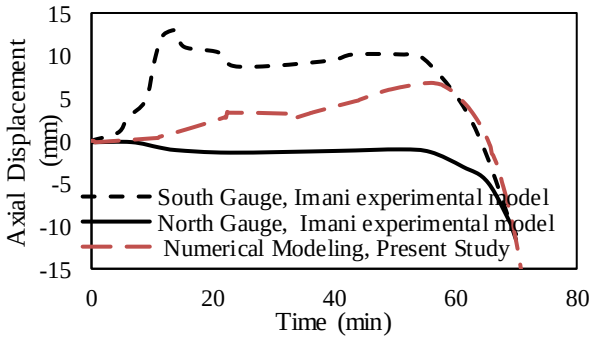

Figure 13. The vertical displacement-time curve in Imani's experimental model and numerical analysis in this study

3.4 Research Parameters

The behavior and especially the failure time in structural elements under fire loading vary in intact and damaged structures. The amount of fire load applied to the structure is an important parameter in the assessment of the behavior of structures under thermal loading. In addition to standard fire load, it is tried to investigate the behavior of structure under a typical natural fire load.

The standard temperature-time curve used in this study was taken according to ISO 834, which follows Equation 10. In this equation, θ_g is the temperature, t is the time in hours and the room temperature is considered 20.

$$\theta_g = 345\log(8t + 1) + 20 \quad (10)$$

In addition to the standard fire load mentioned, typical fire loads caused by gas leak are also assumed for the structure. The fire load with the mean of 345 MJ/m^2 and standard deviation of 262 MJ/m^2 and the normal distribution is considered in the probabilistic analyses for rooms of the frame [3]. Figure 14 shows the temperature-time curves of gas fire load for the means and the mean minus/plus the standard deviation.

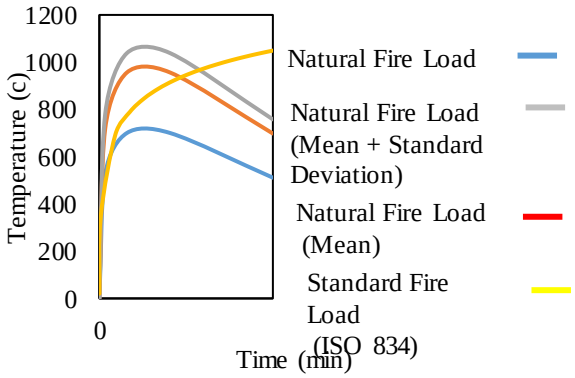

Figure 14. Temperature-time curves for the fire load

Fire loads are converted to the temperature-time curves and then applied to the RC sections in Abaqus software. Finally, the temperature-time curves are derived for the depth of sections and used by OpenSees software. The fc with the mean of 21 MPa and Coefficient of Variation (CoV) of 0.1 and the Log-Normal distribution is used for concrete materials. The f_y with the mean of 338 MPa, CoV of 0.1 and log-normal distribution is considered for steel materials. The dead load is also considered with mean of 600 Kg/m^2, CoV of 0.1 and Normal distribution. Live load considered with Gamma distribution, mean of 200 Kg/m2 and Cov of 0.8 [1, 31, 32]. A uniform distribution with four different cracking patterns is used for cracks at different damage levels. The frame is exposed to thermal load within steps of 0.1 for damage indices of 0 to 0.8. The position of fire is considered separately at the middle span of the first, third and sixth stories. A schematic diagram of this model is presented in Figure 15. It should be noted that the effect of cracks is considered only in the heat distribution in damaged sections.

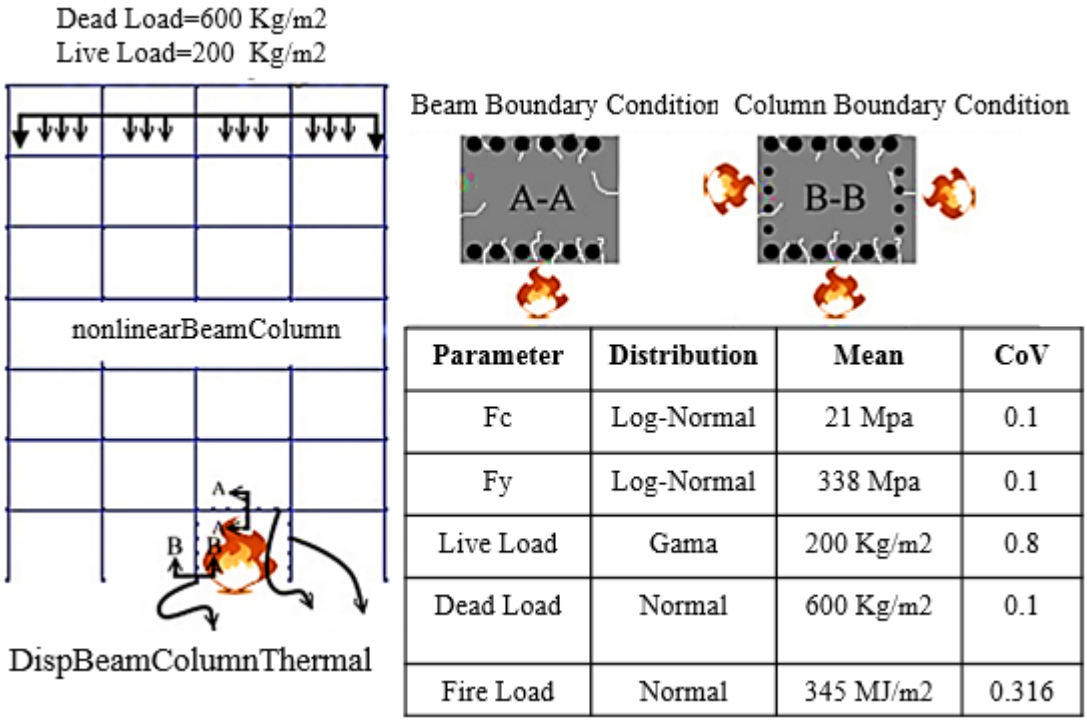

Parameter	Distribution	Mean	CoV
Fc	Log-Normal	21 Mpa	0.1
Fy	Log-Normal	338 Mpa	0.1
Live Load	Gama	200 Kg/m2	0.8
Dead Load	Normal	600 Kg/m2	0.1
Fire Load	Normal	345 MJ/m2	0.316

Figure 15. Model specifications

4. Assessment of Analytical Results

4.1 Deterministic Analysis of RC Frame under Post-damage Fire Loading

Changes in shear force and bending moment in the beams over time and the stress-strain relationship in the columns are used to investigate the behavior of reinforced concrete frame in the region subjected to thermal loading. Figure 16 shows the location of assumed fire loading as well as the temperature versus time curve used to introduce the fire loading to the structure. The stress-strain curves of fibers exposed to the fire in the left column as well as the shear force and bending moment values at the left end of the beam are assessed at different damage levels.

As shown in Figure 16, the shear force and bending moment curves clearly show the occurrence of failure when the damage index is equal to or greater than 0.4. Moreover, the time of the first failure decreases as the frame damage index increases. It is observed that the shear and flexural capacities decrease in the beam as the damage index increases, which leads to a loss of strength under thermal loading.

The stress-strain curves in Figure 16 show that the compressive stress decreases in the concrete fiber of column exposed to the fire load as the damage index is increased. In this fiber, which is exposed to the fire, compressive strength reaches zero at all damage indices, but this happens at a shorter time when higher damage indices are assumed.

The vertical displacement of the beam at midspan can be used as an indicator to evaluate the response and strength of the structure against thermal loads.

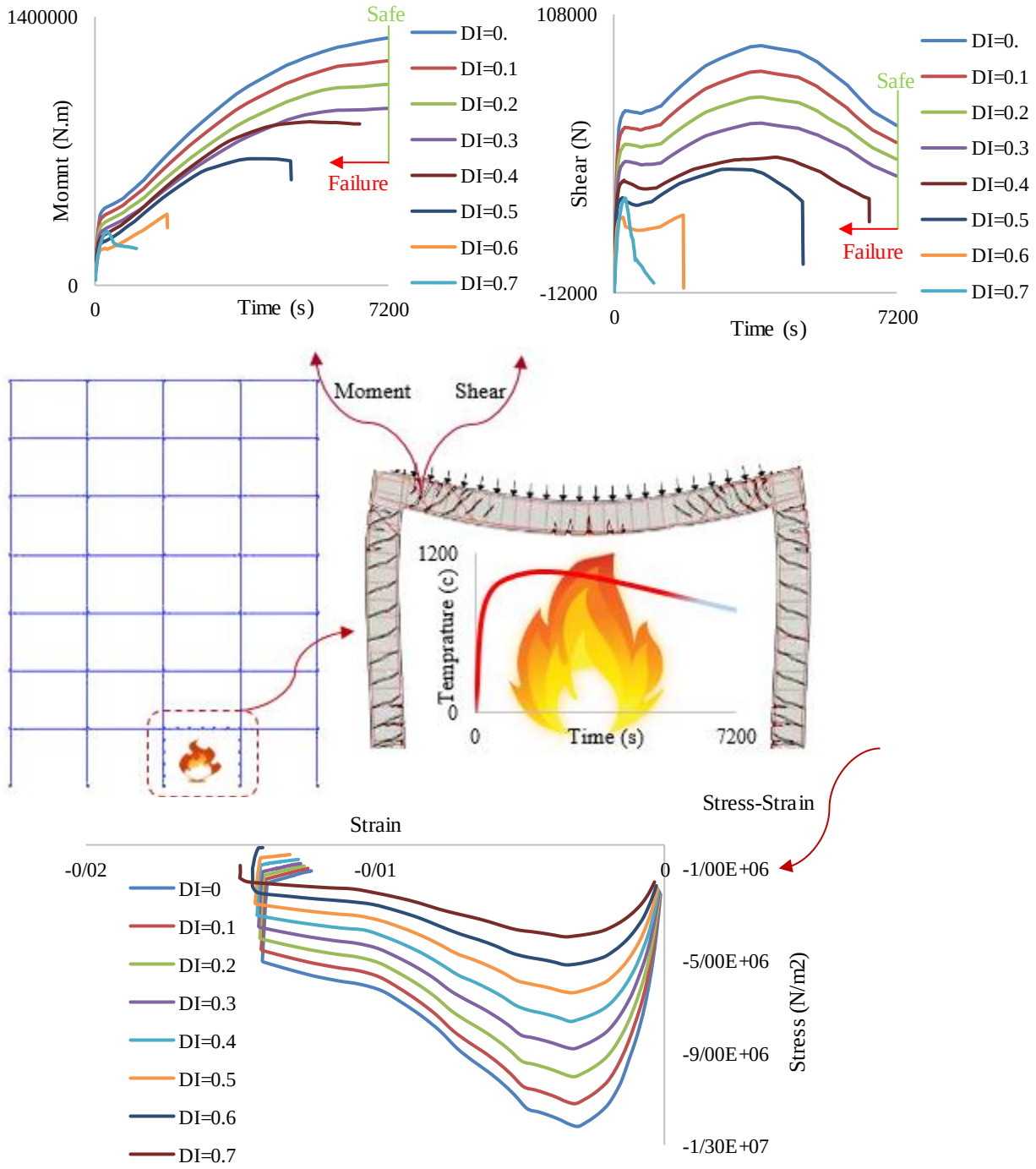

Figure 16. Deterministic analysis of the behavior of the RC frame exposed to a thermal load (Q=600 MJ/m^2)

Using this parameter, a sudden increase in the vertical displacement at midspan can be used to identify failure. For example, Figure 17 shows the midspan vertical displacement in the 6th story under fire condition assuming initial damage indices of 0 and 0.5 at natural fire load of Q=600 MJ/m^2. As can be seen in the figure, the intact frame, with a damage index of zero did not show any abrupt changes in its midspan vertical displacement, whereas the damaged frame demonstrates a sudden increase in its midspan vertical displacement at 4295 second, which indicates failure.

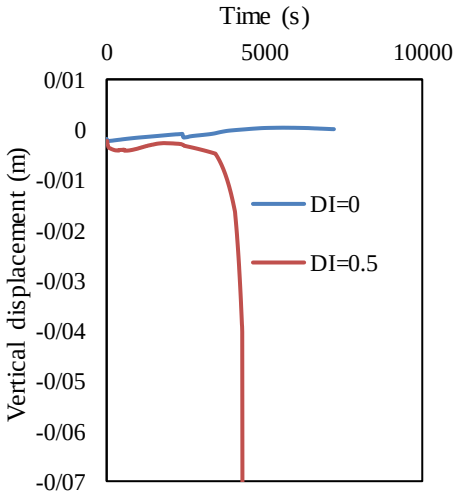

Figure 17. Vertical displacement at midspan under fire in intact and damaged structure (Q=600 MJ/m^2

4.2 Probabilistic Analysis of Failure Time

For probabilistic analysis, f_c, f_y, gravity load, location of fire, and fire load are selected as variables and the mechanical-thermal analysis is conducted separately for each damage level. The Markov-Monte Carlo method is used for probabilistic analysis. Initially, the analysis is done for standard fire loads at different damage levels to evaluate the probability of the first failure at different times using the probabilistic analysis, probabilistic distribution function (PDF) and cumulative distribution function (CDF). In Figure 18, CDF and PDF curves are presented for various damage indices.

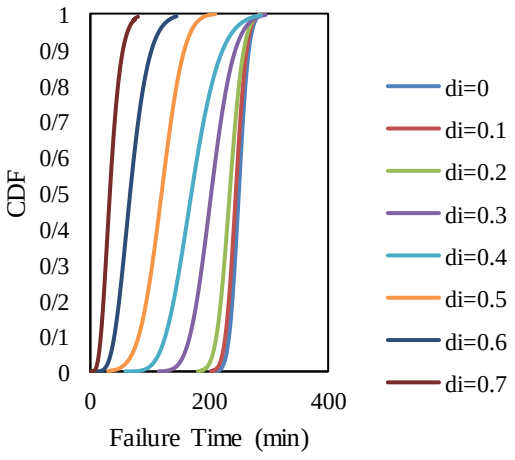

a)

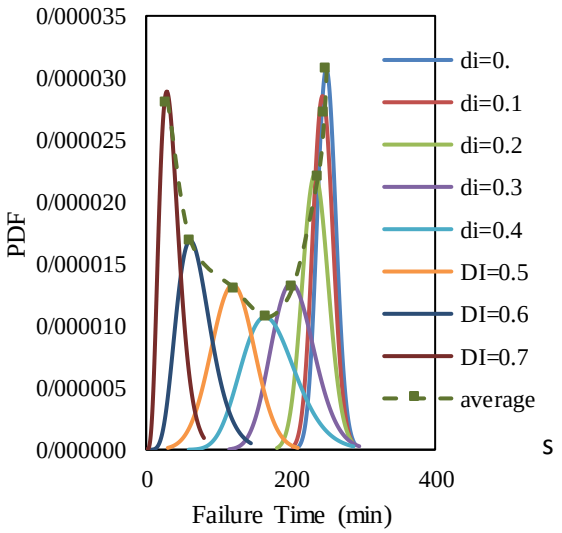

b)

Figure 18. a) CDF curve of failure time; b) PDF curve of failure time for frame elements due to standard fire load

In thermal analysis under standard fire load, it is assumed that the fire load is applied to the spans for 5 hours (300 minutes). The thermal analysis continues until failure occurs in one of the elements of the damaged span due to fire load. Failure time is considered as the time of failure due to standard time-temperature load. In each damage index, a separate probabilistic analysis is performed using the Monte Carlo method. Monte Carlo probability analysis was performed with a maximum sample space of 50000 and a coefficient of variation of 0.001. The objective function in this analysis is the failure time, and the contribution of each failure time is presented as CDF and PDF curves.

The failure probability at any time under standard fire load is expressed as $P[t < T|i-th\ state]$. The results show that as the damage index rises, the failure probability increases in the structure. According to Figure 18, the minimum and maximum probable failure times in the frame assuming a damage index of 0.1 are 216 and 278 minutes, respectively, with a mean value of 247 minutes. This mean value is only 5

minutes longer than the failure time of the intact structure.

Figure 18 also shows that as the damage level increases, the mean of failure time in the reinforced concrete frame decreases. At the damage index of 0.6 and 0.7, the structural resistance to fire is significantly reduced. The mean failure time assuming these indices are 32 and 63 minutes, respectively. The PDF curve interval shows the failure time when the damage index varies between 0 and 0.7. The figure indicates that at high damage indices, the failure time is relatively insensitive to the random variables but in the intermediate range of damage indices (0.3-0.6), the sensitivity of the failure time to random variables is increased.

4-3- RC frame under natural fire loading

Since the standard fire load is an unrealistic load for a structure, a case of a natural fire load was used to evaluate the failure probability of RC frame under fire load. Monte Carlo-Markov method was used to evaluate the probability of failure under fire load at different damage indices. A separate sample space was created for each damage index and the Markov probability chain was formed using the Monte Carlo method.

Figure 19 represents the probabilities of first failure in the 7-story RC frame for different damage levels ($P[failure\ state|i-th\ state]$). The probability of first failure at each damage level represents an array in the last column of the Markov matrix for the post-damage state, as shown in Equation 4. According to this figure, the failure probability at damage indices of 0.1 and 0.2 is equal to zero under the assumed natural gas fire loading for 2 hours. As the damage index is increased, the probability of first failure increases. Failure occurs in all cases with a damage index exceeding 0.7.

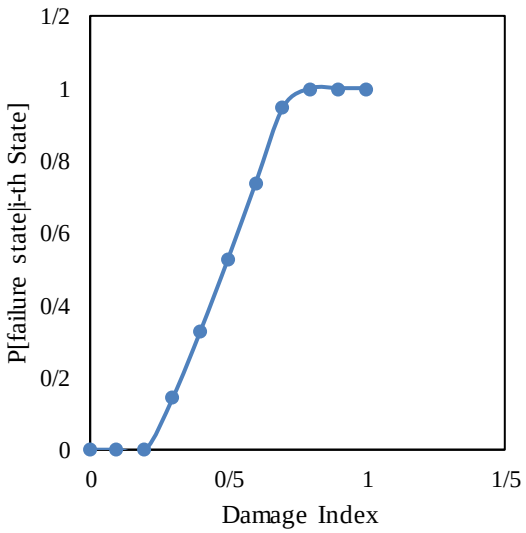

Figure 19. Failure probabilities at each damaged index (last column of Markov matrix in post damaged fire scenarios)

Figure 19 shows a chain of the failure probability of the reinforced concrete frame under natural fire load. Each chain indicates the probability of transition from a specific damage index to the failure level. Matrix P_3 shows the Markov matrix of the failure probability of 7-story reinforced concrete frame under natural fire load. For example, if the reinforced concrete frame has a damage index of 0.6, the probability of failure under natural fire load is calculated as: $P[failure\ |damage\ index = 0.6]$, which is equal to 74 percent.

$$P_3[failure\ State|i-th\ State] = \begin{bmatrix} 0 & 0 & 0 & 0 & 0 & 0 & 0 & 0 & 0 & 0 & 0 \\ 0 & 0 & 0 & 0 & 0 & 0 & 0 & 0 & 0 & 0 & 0 \\ 0 & 0 & 0 & 0 & 0 & 0 & 0 & 0 & 0 & 0 & 0 \\ 0 & 0 & 0 & 0 & 0 & 0 & 0 & 0 & 0 & 0 & 0.145 \\ 0 & 0 & 0 & 0 & 0 & 0 & 0 & 0 & 0 & 0 & 0.33 \\ 0 & 0 & 0 & 0 & 0 & 0 & 0 & 0 & 0 & 0 & 0.53 \\ 0 & 0 & 0 & 0 & 0 & 0 & 0 & 0 & 0 & 0 & 0.74 \\ 0 & 0 & 0 & 0 & 0 & 0 & 0 & 0 & 0 & 0 & 0.94 \\ 0 & 0 & 0 & 0 & 0 & 0 & 0 & 0 & 0 & 0 & 1 \\ 0 & 0 & 0 & 0 & 0 & 0 & 0 & 0 & 0 & 0 & 1 \\ 0 & 0 & 0 & 0 & 0 & 0 & 0 & 0 & 0 & 0 & 1 \end{bmatrix} \quad (11)$$

Figure 20 shows cumulative distribution functions (CDFs) for the time of the first failure at each damage index if any failure occurs. At the damage index of 0.1, the probability of failure within the two hours under investigation is zero. As the damage

index increases, the failure probability increases.

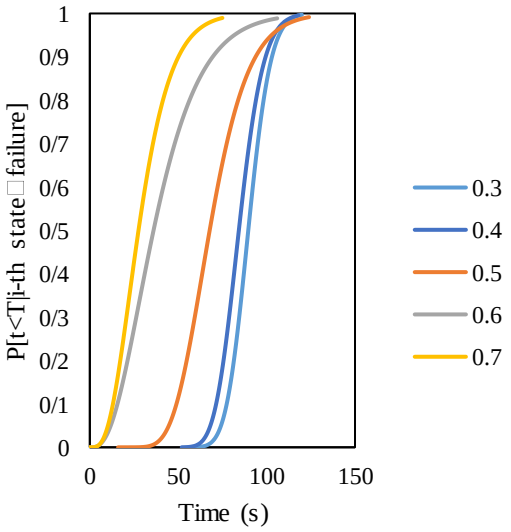

Figure 20. CDFs for the probability of failure time at each damaged index if any failure occurs

If a fire is considered to be a certain event, the failure probability at a given time can be calculated as follows:

For example, the probability that any element in a structure damaged with an index of 0.3 fail within 100 minutes under the natural fire is calculated as Eq 13.

This value is calculated as 0.49 if the damage index is increased to 0.5, which indicates that there is a 49% probability of failure within less than 100 minutes for a fire-exposed RC frame.

If the failure probability is categorized for each damage index at different times, all values of the failure probability can be presented in a matrix. Each row represents the failure probability values for a different damage index, and each column represents the failure probability values at a given time for different indices. Therefore, each row of the matrix represents the $P[failure\ time < t \,|\, i-th\ State\ ] = P_{t,i}$ expression, where i is damage index, which varies between 0, 0.1, 0.2, 0.3, 0.4, 0.5, 0.6, and 0.7, and t is the failure time, which varies between 20, 40, 60, 80, 100, and 120 minutes. The failure probability values for different times and indices are shown in Matrix $P_{i,t}$ (Eq. 14).

$$P[\ t_{failure} < t \,|\, i-th\ State\ ] = P[\ failure\ State \,|\, i-th\ State\ ] \times P[t < T \,|\, i-th\ State \cap failure\ State\ ] \tag{12}$$

$$P[\ t_{failure} < 100 \,|\, i-th\ State = 0.3\ ] = P[failure\ State \,|\, 0.3\ ] \times P[t < 100 \,|\, i-th\ State = 0.3 \cap failure\ State\ ]$$

$$\rightarrow P[\ t_{failure} < 100 \,|\, i-th\ State = 0.3\ ] = 0.145 \times 0.9 = 0.13 \tag{13}$$

$$P_{i,t} = \begin{bmatrix} P_{0,20} & P_{0,40} & P_{0,60} & P_{0,80} & P_{0,100} & P_{0,120} \\ P_{1,20} & P_{1,40} & P_{1,60} & P_{1,80} & P_{1,100} & P_{1,120} \\ P_{2,20} & P_{2,40} & P_{2,60} & P_{2,80} & P_{2,100} & P_{2,120} \\ P_{3,20} & P_{3,40} & P_{3,60} & P_{3,80} & P_{3,100} & P_{3,120} \\ P_{4,20} & P_{4,40} & P_{4,60} & P_{4,80} & P_{4,100} & P_{4,120} \\ P_{5,20} & P_{5,40} & P_{5,60} & P_{5,80} & P_{5,100} & P_{5,120} \\ P_{6,20} & P_{6,40} & P_{6,60} & P_{6,80} & P_{6,100} & P_{6,120} \\ P_{7,20} & P_{7,40} & P_{7,60} & P_{7,80} & P_{7,100} & P_{7,120} \end{bmatrix} = \begin{bmatrix} 0 & 0 & 0 & 0 & 0 & 0 \\ 0 & 0 & 0 & 0 & 0 & 0 \\ 0 & 0 & 0 & 0 & 0 & 0 \\ 0 & 0 & 0.001 & 0.016 & 0.129 & 0.145 \\ 0 & 0 & 0.0016 & 0.12 & 0.31 & 0.33 \\ 0 & 0.005 & 0.17 & 0.4 & 0.5 & 0.53 \\ 0.02 & 0.11 & 0.42 & 0.62 & 0.7 & 0.74 \\ 0.05 & 0.24 & 0.75 & 0.89 & 0.94 & 0.94 \end{bmatrix} \tag{14}$$

The probability values in the last column of the matrix $P_{i,t}$ are the same as the probability values in the last column of the Markov matrix.

4.4 RC frame under natural fire loading with uncertain damage index

A specific damage index was used in the preceding sections. However, the damage

index in an existing reinforced concrete frame may be unknown. To consider the uncertainty of the damage index in the reinforced concrete frame exposed to fire, a uniform distribution was considered for the damage index and a sample space containing random variables was created. A Monte Carlo analysis was then performed and the probability distribution of failure time was calculated. In this analysis, random variables include damage indices with a uniform distribution between 0 and 0.7, in addition to the random variables already considered. All random variables were placed in a sample space.

Figure 21 shows the sample space of failure time found as a result of the Monte Carlo analysis, which consists of 53000 failure times. Fig. 22 shows the CDF curve of the failure time if the damage to the reinforced concrete frame is taken as one of the random variables. For example, the figure shows that there is a 20 percent probability that the failure time is less than 85 min. According to this figure, about 32% of the sample space points represent failure before 7200 s. The other 68% of sample space points remained safe until 7200 s.

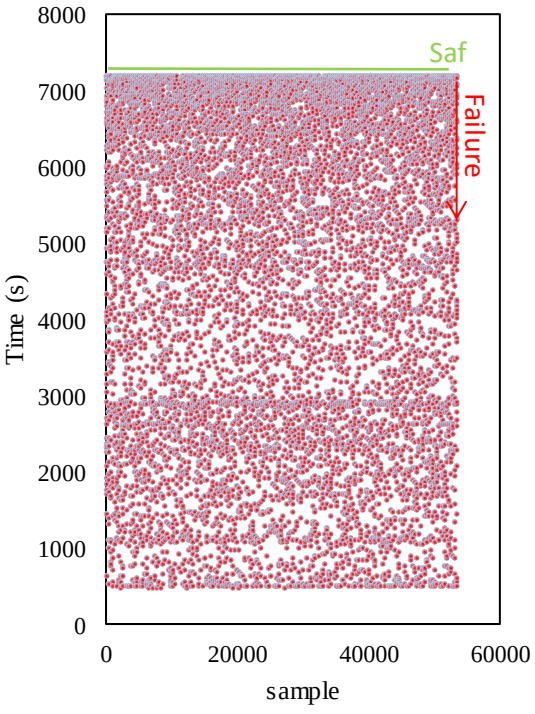

Figure 21. Sample space for failure time

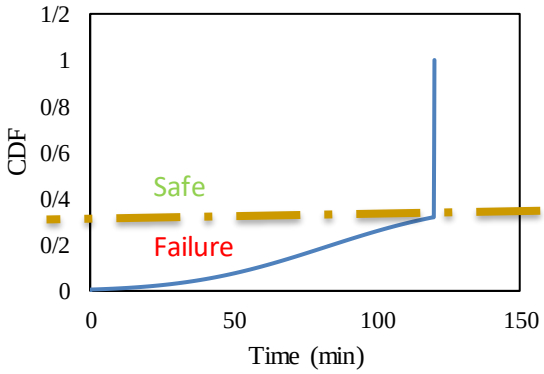

Figure 22. Failure time cumulative distribution function

5. Conclusions

This study aimed to investigate the failure probability in a damaged reinforced concrete frame exposed to fire. A 7-story RC frame was considered for the probabilistic analysis. The Monte Carlo-Markov method was used to assess the failure probability at different damage indices. A variety of damage indices were applied to the structure and the failure probability of RC frame was then evaluated in regard to the strength loss and effect of cracking and spalling.

The resistance of intact RC frame under fire loading was found to be notably different from that of the damaged RC frame, with a greater damage resulting in greater differences, as expected. The results of the probabilistic analysis indicate that the failure probability of RC frame elements under the considered natural fire loading is almost zero at low damage indices (0, 0.1, and 0.2), indicating that the frame has the capacity to withstand the fire load. The probability of failure increased with an increase in the damage index. As the damage index is increased, the strength loss of elements, increased cracking and spalling of concrete cover result in an increased failure probability due to the thermal load. The failure probability was calculated as 0.33 and 0.53 at damage indices of 0.4 and 0.5, respectively. The failure time decreased as damage index increased. If any failure occurs, the range of failure time decreases as damage index increases in the RC frame.

The framework developed in this paper is of great value to investigations in which the aim

is to assess the performance of a damaged structure that is later exposed to fire loading.

References

1. Moradi, M., H. Tavakoli, and G. AbdollahZade,(2019) Sensitivity analysis of the failure time of reinforcement concrete frame under postearthquake fire loading. *Structural Concrete*.
2. Tavakoli, H. and M.M. Afrapoli,(2018) Robustness analysis of steel structures with various lateral load resisting systems under the seismic progressive collapse. *Engineering Failure Analysis*. *83*, p. 88-101.
3. Khorasani, N.E., T. Gernay, and M. Garlock,(2017) Data-driven probabilistic post-earthquake fire ignition model for a community. *Fire safety journal*. *94*, p. 33-44.
4. Moradi, M. and M. Abdolmohammadi,(2020) Seismic fragility evaluation of a diagrid structure based on energy method. *Journal of Constructional Steel Research*. *174*, p. 106311.
5. Moradi, M., H. Tavakoli, and G. Abdollahzadeh,(2019) Probabilistic assessment of failure time in steel frame subjected to fire load under progressive collapses scenario. *Engineering failure analysis*. *102*, p. 136-147.
6. Zhong, H., G. Chen, and S. Jiang,(2016) A novel method for evaluation of fire prevention by using water curtain with large droplets. *Journal of Loss Prevention in the Process Industries*. *43*, p. 585-592.
7. Mousavi, S., A. Bagchi, and V.K. Kodur,(2008) Review of post-earthquake fire hazard to building structures. *Canadian Journal of Civil Engineering*. *35*(7), p. 689-698.
8. Zolfaghari, M., E. Peyghaleh, and G. Nasirzadeh,(2009) Fire following earthquake, intra-structure ignition modeling. *Journal of fire sciences*. *27*(1), p. 45-79.
9. Alderighi, E. and W. Salvatore,(2009) Structural fire performance of earthquake-resistant composite steel–concrete frames. *Engineering Structures*. *31*(4), p. 894-909.
10. Keller, W.J. and S. Pessiki,(2012) Effect of earthquake-induced damage to spray-applied fire-resistive insulation on the response of steel moment-frame beam-column connections during fire exposure. *Journal of Fire Protection Engineering*. *22*(4), p. 271-299.
11. Memari, M., H. Mahmoud, and B. Ellingwood,(2014) Post-earthquake fire performance of moment resisting frames with reduced beam section connections. *Journal of Constructional Steel Research*. *103*, p. 215-229.
12. Albuquerque, G.L., et al.,(2018) Behavior of thermally restrained RC beams in case of fire. *Engineering Structures*. *174*, p. 407-417.
13. Pucinotti, R., O. Bursi, and J.-F. Demonceau,(2011) Post-earthquake fire and seismic performance of welded steel–concrete composite beam-to-column joints. *Journal of constructional steel research*. *67*(9), p. 1358-1375.
14. Lou, T., W. Wang, and B.A. Izzuddin,(2023) A framework for performance-based assessment in post-earthquake fire: Methodology and case study. *Engineering Structures*. *294*, p. 116766.
15. Risco, G., V. Zania, and L. Giuliani,(2023) Numerical assessment of post-earthquake fire response of steel buildings. *Safety science*. *157*, p. 105921.
16. Khiali, V. and H. Rodrigues,(2023) Experimental Evaluation of Post-Earthquake Fire on Reinforced Concrete Structures—A Review. *CivilEng*. *4*(2), p. 469-482.
17. Black, M., A.T. Brint, and J. Brailsford,(2005) A semi-Markov approach for modelling asset deterioration. *Journal of the Operational Research Society*. *56*(11), p. 1241-1249.
18. Kanjilal, O. and C. Manohar,(2015) Markov chain splitting methods in structural reliability integral estimation. *Probabilistic Engineering Mechanics*. *40*, p. 42-51.
19. Khorasani, N.E., M. Garlock, and P. Gardoni,(2014) Fire load: Survey data, recent standards, and probabilistic models for office buildings. *Engineering Structures*. *58*, p. 152-165.
20. Park, Y.-J. and A.H.-S. Ang,(1985) Mechanistic seismic damage model for reinforced concrete. *Journal of structural engineering*. *111*(4), p. 722-739.
21. Choi, H., et al.,(2016) Seismic response estimation method for earthquake-damaged RC buildings. *Earthquake Engineering & Structural Dynamics*. *45*(6), p. 999-1018.
22. EN1992-1-1,(2004) Eurocode 2: Design of concrete structures-Part 1-2: General rules-structural fire design. *European Committee for Standardization*.
23. Behnama, B. and H.R. Ronagh,(2013) Post-earthquake fire performance-based behavior of reinforced concrete structures. *Earthquakes and Structures*. *5*(4), p. 379-394.
24. Wen, B., B. Wu, and D. Niu,(2016) Post-earthquake fire performance of reinforced concrete columns. *Structure and Infrastructure Engineering*. *12*(9), p. 1106-1126.
25. Usmani, A., et al.,(2012) Using opensees for structures in fire. *Journal of Structural Fire Engineering*. *3*(1), p. 57-70.
26. Jiang, J. and A. Usmani,(2013) Modeling of steel frame structures in fire using OpenSees. *Computers & Structures*. *118*(1), p. 90-99.
27. Taerwe, L., et al.,(2008) fib bulletin 46: Fire Design of Concrete Structures–Structural Behaviour and Assessment. *State-of-the art Report, International Federation for Structural Concrete (fib TG 4.3. 2), Lausanne, Switzerland*.
28. Jason, L., et al.,(2006) An elastic plastic damage formulation for concrete: Application to elementary tests and comparison with an isotropic damage model. *Computer methods in applied mechanics and engineering*. *195*(52), p. 7077-7092.
29. Kamath, P., et al.,(2015) Full-scale fire test on an earthquake-damaged reinforced concrete frame. *Fire Safety Journal*. *73*, p. 1-19.
30. Imani, R., G. Mosqueda, and M. Bruneau,(2014) Experimental study on post-

earthquake fire resistance of ductile concrete-filled double-skin tube columns. *Journal of Structural Engineering*. *141*(8), p. 04014192.
31. Guo, Q. and A.E. Jeffers,(2014) Finite-element reliability analysis of structures subjected to fire. *Journal of Structural Engineering*. *141*(4), p. 04014129.
32. Parisi, F., M. Scalvenzi, and E. Brunesi,(2019) Performance limit states for progressive collapse analysis of reinforced concrete framed buildings. *Structural Concrete*. *20*(1), p. 68-84.